Acta Mech Sin (2007) 23:597–607
DOI 10.1007/s10409-007-0101-6

RESEARCH PAPER

Validity ranges of interfacial wave theories in a two-layer fluid system

Yutang Yuan · Jiachun Li · Youliang Cheng

Received: 4 January 2007 / Revised: 9 May 2007 / Accepted: 5 June 2007 / Published online: 4 September 2007

Abstract In the present paper, we endeavor to accomplish a diagram, which demarcates the validity ranges for interfacial wave theories in a two-layer system, to meet the needs of design in ocean engineering. On the basis of the available solutions of periodic and solitary waves, we propose a guideline as principle to identify the validity regions of the interfacial wave theories in terms of wave period T, wave height H, upper layer thickness d_1, and lower layer thickness d_2, instead of only one parameter–water depth d as in the water surface wave circumstance. The diagram proposed here happens to be Le Méhauté's plot for free surface waves if water depth ratio $r = d_1/d_2$ approaches to infinity and the upper layer water density ρ_1 to zero. On the contrary, the diagram for water surface waves can be used for two-layer interfacial waves if gravity acceleration g in it is replaced by the reduced gravity defined in this study under the condition of $\sigma = (\rho_2 - \rho_1)/\rho_2 \to 1.0$ and $r > 1.0$. In the end, several figures of the validity ranges for various interfacial wave theories in the two-layer fluid are given and compared with the results for surface waves.

Keywords Validity ranges · Two-layer fluid · Interfacial waves · Interfacial solitary waves · Ursell number

1 Introduction

The ocean is not homogeneous in both temperature and salinity. The phenomenon ultimately leads to the density stratification in the ocean, among which the two-layer system represents the most typical one with intense density variation. The study of internal waves is of primarily importance in the ocean acoustics, marine ecology and physical oceanography. Internal waves traveling in the interior of the ocean water body tend to carry enormous energy, which may seriously do harm to ocean structures, such as deep-sea drilling rigs, drillers and vertical pipes [1]. For the sake of safety considerations, those ocean structures are required to withstand huge wave forces and moments that exerted by large amplitude internal waves [2]. As for hazard internal wave performance, there are two events in record. The first is in 1980, a working drilling machine in the Andaman Sea was apparently spun through 90° and carried 100 feet away by internal solitary waves [3]. The other happened in the northern South China Sea, a fixed oil tank swayed 110° in less than 5 min when a group of internal waves passing by [4]. These incidents imply that the internal wave factors are important in ocean engineering.

While designing deep ocean structures, engineers should know in advance the characteristics and details of the flow field induced by the internal waves. Since the instantaneous wave force differs tremendously under different ocean wave climate conditions. At present time, there are at least seven

The project supported by the Knowledge Innovation Project of CAS (KJCX-YW-L02), the National 863 Project of China (2006AA09A103-4), China National Oil Corporation in Beijing (CNOOC), and the National Natural Science Foundation of China (10672056).

Y. Yuan (✉) · J. Li
Division of Engineering Sciences, Institute of Mechanics, Chinese Academy of Sciences, Beijing 100080, China
e-mail: yuanyutang@imech.ac.cn

J. Li
e-mail: jcli05@imech.ac.cn

Y. Cheng
Department of Dynamic Engineering, North China Electric Power University, Baoding 071003, China
e-mail: ylcheng001@163.com

wave theories available for the internal waves in a two-layer system, such as linear theory, the second to the fifth order internal Stokes wave theories, internal solitary wave and cnoidal wave theories. Therefore, it is a chanllenge for us to choose the suitable internal wave theories when calculating wave force.

Up to now, the issue for the surface wave theories has been fully resolved. Traditionally, there are three categories of surface waves, namely, the small amplitude waves, the finite amplitude waves and the long waves or shallow water waves, which transport different amounts of energy and exert different wave forces on ocean structures. Le Méhauté [5] has worked out a diagram for "limits of validity for various surface wave theories" providing the criteria of the validity ranges for various water surface waves. The chart has been proved to fit well by the tests of Yuen [6] and Chakrabarti [7] in laboratory experiments. And then, Iwagaki [8] presented his study, only indicating the applicability ranges of the linear theory, the third order Stokes theory and the cnoidal theory. As for internal waves, so far we still have no similar diagram serving as the guidelines to be used in engineering design. As a matter of fact, the free surface wave can also be regarded as a two-layer system with a large apparent density difference. In contrast, the oceanic interfacial waves in the ocean interior usually propagate on the thermocline with a small density difference (around 0.1%, thus minor disturbances can result in billow). Furthermore, besides wave height H and period T, the depth ratio r of the upper and lower layers becomes an additional parameter in demarcating different validity ranges.

It is helpful to survey the recent development of internal wave theories, on which our validity range study is based, during the last three decades. Generally speaking, the propagation of internal solitary waves is described by $K\mathrm{d}V$ equation, whereas we need a revised form for the critical situation as the upper and lower layer depths are close. If the density variation occurs merely in the upper layer, we may use the intermediate long wave theory, which turns into the so-called Benjamin-Ono equation if the lower depth becomes infinity. In the meantime, the two-dimensional weak solitary wave is formulated by KP (Kadomtsev–Patviashivilli) equation. By extending Fenton's Stokes wave theory, Cheng and Li [9] obtained the fifth order interfacial wave results with the help of Mathematica based on the stream function formulation. Lamb [10] studied the limiting forms of extreme internal solitary waves in the ocean by using the two-layer model evolution equations. For highly nonlinear internal solitary waves, Helfrich and Melville [11] showed that the limiting flat-crested wave for a Boussinesq fluid has the same amplitude as that found by Miyata–Choi–Camassa [12,13], and the solitary waves are nearly indistinguishable from the fully nonlinear theory over a wide range of relative layer depths [14]. Grue [15] studied the breaking and broadening of the internal solitary waves in a two-layer system, finding that the nondimensional fluid velocity u/c increases almost linearly with the wave amplitude and when $H/d_{\mathrm{thin}} = 0.855$ (d_{thin} is the less of d_1 and d_2), the fluid velocity at the wave peak is equal to the phase speed. For periodic breaking waves, Fringer and Street [16] performed numerical simulations to study the extreme amplitude of interfacial waves by imposing a source term in the horizontal momentum equation. They are able to get a greater steepness than usual value of $kH = 0.74$ (where $k = 2\pi/L$ is the wavenumber) before it breaks by increasing the interface thickness. This steepness is asymptotic to the inviscid limit of $kH = 1.1$ [17] or 1.05 if the effect of background shear is considered [16].

The purpose of the present study are: (1) to determine the validity ranges for various two-layer internal waves; (2) to find the bordering lines between these theories; (3) to discuss the effects of the water depth ratio and densities; and (4) to find the correlations between the surface waves and the two-layer interfacial waves.

2 Wave equations and their solutions

Now we are considering the traveling periodic waves in a two-layer fluid on a horizontal impermeable bed, which can be regarded as a steady flow if the coordinate system moves at the same speed as the wave. The water is assumed incompressible and bounded by two rigid walls at the upper and lower boundaries. Although the natural oceans are actually open, if the upper layer thickness is deep enough as compared to the amplitude of interfacial wave, the rigid lid approximation seems to be reasonable. The experimental evidence reported by Kao et al. [18] supports the rigid-lid approximation. It was also verified and applied by Benney [19] and Pelinovskiy [20] in their theoretical study of internal waves. However, there are surface waves in the open area. The wave–current or wave (surface)–wave (internal) interaction should be considered when the water depth ratio is small enough [21,22]. Then, the origin is set on the plane of water surface, with x as the horizontal coordinate and z as the vertical coordinate (Fig. 1).

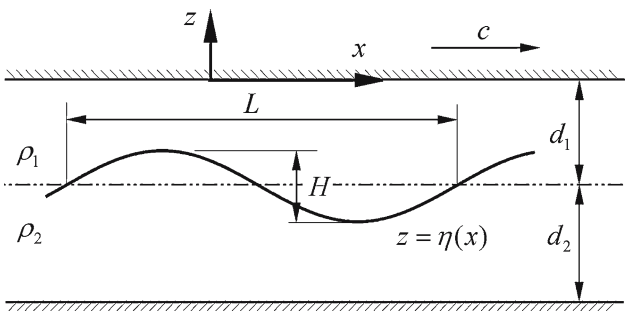

Fig. 1 The coordinate system of two-layer fluid interfacial waves, the origin is located at the water surface, the densities of the two layers are ρ_1 and ρ_2 and the depths are d_1 and d_2

To facilitate the solution of the problem, we prefer the stream function formulation such that velocity components (u_1, v_1) and (u_2, v_2) are given by $u_1 = \partial\psi_1/\partial z$, $v_1 = -\partial\psi_1/\partial x$, and $u_2 = \partial\psi_2/\partial z$, $v_2 = -\partial\psi_2/\partial x$ if the motion is irrotational, the stream functions ψ_1 and ψ_2 satisfy the Laplace equation throughout the two fluids. Thus

$$\frac{\partial^2\psi_1}{\partial x^2} + \frac{\partial^2\psi_1}{\partial z^2} = 0, \tag{1}$$

$$\frac{\partial^2\psi_2}{\partial x^2} + \frac{\partial^2\psi_2}{\partial z^2} = 0. \tag{2}$$

The upper boundary condition is

$$\psi_1(x, 0) = 0. \tag{3}$$

The bottom boundary conditions is

$$\psi_2(x, -d_1 - d_2) = 0. \tag{4}$$

On the free interface $z = \eta(x)$, the kinematics boundary condition is

$$\psi_2[x, -d_1 + \eta(x)] = -Q, \tag{5}$$

where Q is a positive constant, denoting the total volume rate of flow underneath the stationary wave per unit length normal to the (x, z) plane; and the condition requiring pressure on the free surface to be constant, combined with Bernoulli's equation, that is

$$\begin{aligned}&\frac{1}{2}[(\partial_x\psi_2)^2 + (\partial_z\psi_2)^2] + g[-d_1 + \eta(x)]\\ &- R - (1-\sigma)\left\{\frac{1}{2}\left[(\partial_x\psi_1)^2 + (\partial_z\psi_1)^2\right]\right.\\ &\left. + g[-d_1 + \eta(x)] - R\right\} = 0,\end{aligned} \tag{6}$$

where g is the gravitional acceleration, R is a positive constant, and $\sigma = (\rho_2 - \rho_1)/\rho_2$ is the water density difference ratio.

The following expansion for ψ_1 and ψ_2 are assumed

$$\begin{aligned}\frac{k\psi_1}{\bar{u}} &= -k(z + d_1 + d_2)\\ &\quad + \sum_{i=1}^{\infty}\sum_{j=1}^{i}\varepsilon^i F_{1ij}\sinh(jkz)\cos(jkx),\end{aligned} \tag{7}$$

$$\begin{aligned}\frac{k\psi_2}{\bar{u}} &= -k(z + d_1 + d_2)\\ &\quad + \sum_{i=1}^{\infty}\sum_{j=1}^{i}\varepsilon^i F_{2ij}\sinh(jkz)\cos(jkx),\end{aligned} \tag{8}$$

$$k\eta(x) = \sum_{i=1}^{\infty}\sum_{j=1}^{i} B_{ij}\varepsilon^i\cos(jkx), \tag{9}$$

in which $\bar{u}$ is the mean fluid speed for any constant value of z, and $k = 2\pi/L$ is the wavenumber.

Now, the perturbation expansion in terms of $\varepsilon = kH/2$ can be assumed for the quantities in these equations, in which the undisturbed state is a uniform flow of d_1, d_2, and speed $c_0(g/k)^{1/2}$

$$\bar{u}\left(\frac{k}{g}\right)^{1/2} = c_0 + \sum_{i=1}^{\infty} c_i\varepsilon^i, \tag{10}$$

$$Q\sqrt{\frac{k^3}{g}} = \bar{u}\sqrt{\frac{k^3}{g}}d_2 + \sum_{i=1}^{\infty} D_i\varepsilon^i, \tag{11}$$

$$\frac{Rk}{g} = \frac{1}{2}c_0 - kd_1 + \sum_{i=1}^{\infty} E_i\varepsilon^i. \tag{12}$$

The coefficients in these equations (F_{1ij}, F_{2ij}, B_{ij}, c_0, c_i, D_i, E_i) are all dimensionless.

The dispersion relation of the steady internal waves in the two-layer fluid can be obtained as

$$\frac{\omega}{\sqrt{gk}} = c_0 + \varepsilon c_1 + \varepsilon^2 c_2 + \varepsilon^3 c_3 + \varepsilon^4 c_4, \tag{13}$$

in which $\omega = 2\pi/T$ is the angular velocity.

3 Validity ranges for two-layer fluid interfacial periodic waves

The elevation profile for the two-layer interfacial waves is expressed as

$$\begin{aligned}k\eta(x) &= \varepsilon\cos(kx) + \varepsilon^2 B_{22}\cos(2kx)\\ &\quad + \varepsilon^3 B_{33}[\cos(3kx) - \cos(kx)]\\ &\quad + \varepsilon^4[B_{42}\cos(2kx) + B_{44}\cos(4kx)]\\ &\quad + \varepsilon^5[-(B_{53} + B_{55})\cos(kx) + B_{53}\cos(3kx)\\ &\quad + B_{55}\cos(5kx)] + 0(\varepsilon^6),\end{aligned} \tag{14}$$

where $\eta(x), k, \varepsilon$ are the wave displacement, the wavenumber and the perturbation parameter, respectively, B_{22}, B_{33} and B_{42}, etc., are functions of σ, kd_1 (or depth ratio r) and kd_2, which are lengthy and intricate expressions. For instance, B_{22} can be expressed in the form of d_2 and r as

$$\begin{aligned}B_{22} = (&c_0^2(\sigma\cosh(kd_2(2-3r))\\ &+ (3\sigma - 4)\cosh(kd_2(r-2)) + 4\cosh(rkd_2)\\ &- 8\sigma\cosh(rkd_2) + 4\cosh(3rkd_2)\\ &- 6\cosh(kd_2(r+2)) + 5\sigma\cosh(kd_2(r+2))\\ &+ 2\cosh(kd_2(3r+2))\\ &- \sigma\cosh(kd_2(3r+2))\coth(kd_2)\mathrm{csch}(rkd_2))\\ &(4(\sigma\cosh(2kd_2(r-1)) - \sigma\cosh(2kd_2(r+1))\\ &+ 2c_0^2(\sigma\sinh(2kd_2(r-1))\\ &- (\sigma - 2)\sinh(2kd_2(r+1))))),\end{aligned} \tag{15}$$

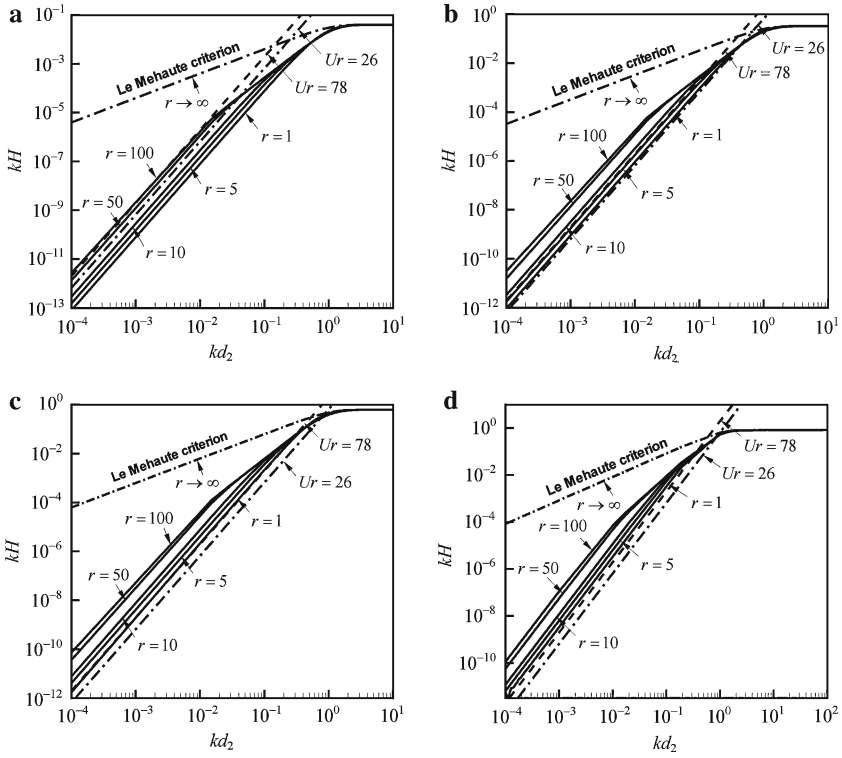

Fig. 2 The maximum amplitude for various periodic waves when $r = 1.0$, 5.0, 10.0, 50.0, 100.0 and ∞. **a**–**d** Are the linear theory, second to fourth order theories accordingly, and the Le Méhauté's criterion corresponds to $r \to \infty$. The maximum amplitude lines are cut off by $Ur = 78$ (*dashed*)

where c_0 is the phase speed and can be written as

$$c_0 = \sqrt{\frac{\sigma \tanh(kd_2) \cdot \tanh(rkd_2)}{\tanh(rkd_2) + (1-\sigma) \cdot \tanh(kd_2)}}. \tag{16}$$

Equation (14) shows that the actual wave elevation contains the higher order harmonic components and results in steeper wave crest and flatter wave trough. For linear theory with the small amplitude, it seems possible to ignore the second term in the expression of the wave profile, when the absolute value of the amplitude of the second term is, say, less than 1.0% of the first term, (when $B_{22} > 0$, +1.0% is taken; when $B_{22} < 0$, −1.0% is taken and when $B_{22} \to 0$, the higher order item becomes more important)

$$\varepsilon |B_{22}| \leq 0.01. \tag{17}$$

3.1 Le Méhauté criterion of maximal periodic wave amplitude

By introducing B_{22} into Eq. (17) with $r \geq 1.0$ and $\sigma \to 0$, we find that kH should satisfy the following expression for linear theory no matter what value r is

$$kH \leq 0.04 \cdot \tanh(kd_2). \tag{18}$$

For the second order waves, we obtain the approximate expression of wave profile as

$$k\eta(x) = \varepsilon \cos(kx) + \varepsilon^2 B_{22} \cos(2kx) + \varepsilon^3 B_{33}(\cos(3kx) - \cos(kx)) + 0(\varepsilon^4). \tag{19}$$

In the same way, when the absolute value of the third order term in the expression of Eq. (19) is small enough compared with the first term, say, less than 1.0%, we get for all $r \geq 1.0$

$$kH \leq 0.366 \cdot \tanh(kd_2). \tag{20}$$

It should be pointed out that the present amplitude of the second item in Eq. (9) is not 0.01 times of the first term any longer; it plays a more important role than the third one to make wave steeper or flatter. In the same way, we can also get the maximal wave steepness of the third order waves as

$$kH \leq 0.6215 \cdot \tanh(kd_2). \tag{21}$$

And for the fourth order

$$kH \leq 0.837 \cdot \tanh(kd_2). \tag{22}$$

When $r \geq 1.0$, those curves are shown in Fig. 2. The dash-dot lines are drawn according to Eqs. (18) and (20)–(22), which are the same as Le Méhauté's criterion for surface waves (here we call it the Le Méhauté's criterion). We notice that it is a logarithmic coordinate, which amplifies the difference of those lines of small kd_2; the dash-dot lines actually are rather close to the solid and long dash-doted lines, which represent the maximal wave slope of different r. It means that Le Méhauté's criterion is true for all $r \geq 1.0$.

When $r < 1.0$, the values of B_{22}, B_{33} etc. are sometimes negative, which may lead to the results that the wave becomes down-ward steeper and up-ward flatter and we call it "the wave polarity changes" just like the internal solitary waves

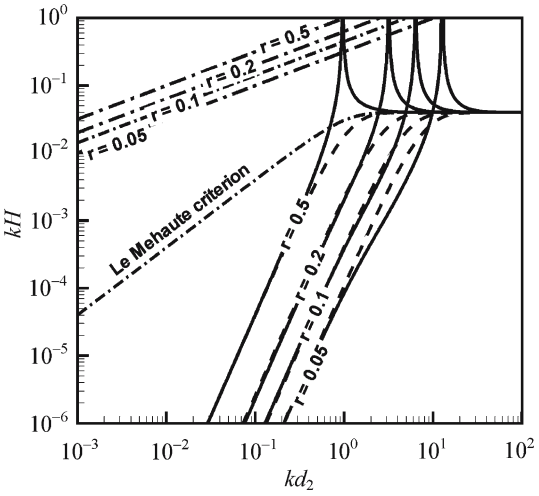

Fig. 3 The maximal amplitude (solid lines) for linear periodic wave theory when $r = 0.05$, 0.1, 0.2 and 0.5. The dashed lines indicate Eq. (24) which are approximate solutions to the solid lines. The dashdot-lines show that the maximum wave heights can not exceed the upper-layer thickness (Using the linear theory as an example)

do. So, the absolute sign in Eq. (17) plays its role. Those parameters "Bs" are functions of kd_2. When they approach to 0, the higher order harmonic waves in the wave elevation are unnegligible. Thus, the higher order theory is an appropriate choice, e.g., in Eq. (19), when $B_{22} \to 0$, B_{33} then becomes dominant. Figure 3 shows that for all $r < 1.0$, Eqs. (18) and (20–22) are also kept valid. Therefore, Le Méhauté's criterion is a rather loose criterion to meet all depth ratio r.

3.2 A more precise criterion

Although the difference between the lines in Figs. 2 and 3 is actually very small, there still exist more precise ways to replace Le Méhauté's criterion. When $r \geq 1.0$, B_{22} is positive, for the linear theory, Eq. (17) can be simplified as Eq. (23) to replace Eq. (18). The difference between Eq. (18) and Eq. (23) is that the first wave slope is irrelevant to r and the second is the function of both r and kd_2, for a given two-layer fluid, Eq. (23) seems to satisfy the maximal wave slope definition better. For the higher order waves, we can use $\varepsilon^{\tau}|B_{ii}| \leq 0.01$ to replace Eqs. (18) and (20–22), where $\tau = 1$, 2, 3 and 4 and $ii = 11$, 22, 33 and 44 for the first to the fourth order periodic wave theories, respectively (see Fig. 2a–d). In the same way, when $r \to \infty$, Le Méhauté's criterion will be resumed

$$kH \leq 0.02/B_{22}. \tag{23}$$

When $r < 1.0$, the value of B_{22} may become negative, which implies the wave polarity changes, and when $B_{22} \to 0$, the higher order term in Eq. (14) is more important. For linear wave, we have $kH \leq 0.02/|B_{22}|$. Now, let Eq. (24) replace Eqs. (18) and (20–22), by changing the values of α and β, we can get a series of smooth lines to approach to the actual, rugged lines of maximal wave slope kH (see Fig. 3, the dashed lines, Eq. (24) is also used in Fig. 8),

$$kH \leq (kH)_{\max} \cdot \tanh^{\alpha}(\beta k d_2). \tag{24}$$

We found that when $r = 0.01$, 0.02, 0.03, 0.05, 0.1, 0.2 and 0.5, and β takes the values listed in Table 1, all $\alpha = 3.0$ (see Fig. 3, the dashed lines).

3.3 A reduced coefficient method

For a long time, people have thought the surface waves are actually one kind of interfacial waves in an air-water system with $\rho_1 \to 0$, and ρ_2 being the water density. The differences between them are their gravity acceleration and larger upper layer thickness. Therefore, we may probably find some relation between them. For surface wave situation, the Boussinesq parameter $\gamma_s = (\rho_2 - \rho_1)/(\rho_2 + \rho_1) \to 1.0$. The dispersion relation for linear surface waves is

$$\omega^2 = gk \tanh(kd). \tag{25}$$

Supposing that the thickness of the air on top of the free surface is r times of the water depth d, and let $f(kd) = \tanh(kd)/\tanh(rkd)$, we have

$$\omega^2 = \frac{\rho_2 - \rho_1}{\rho_2 + f(kd) \cdot \rho_1} gk \cdot \tanh(kd), \tag{26}$$

which is nothing but the same dispersion relation as the linear interfacial waves' [see Eq. (28)]; we define a non-dimensional reduced gravity acceleration as

$$g' = \frac{\rho_2 - \rho_1}{\rho_2 + f(kd) \cdot \rho_1} g = \delta g. \tag{27}$$

With the help of Eqs. (26) and (27), the surface wave dispersion relation can be used for the two-layer interfacial waves. Of course, the way is approximate in some degree for

Table 1 Values of non-dimensional parameter β in Eq. (24) for different waves

Wave theory	$r = 0.01$	$r = 0.02$	$r = 0.03$	$r = 0.05$	$r = 0.1$	$r = 0.2$	$r = 0.5$
1st Order	0.05	0.08	0.1	0.14	0.22	0.40	1.00
2nd Order	0.05	0.08	0.11	0.15	0.24	0.41	1.10
3rd Order	0.05	0.09	0.12	0.17	0.28	0.45	1.20
4th Order	0.06	0.1	0.13	0.19	0.30	0.50	1.30

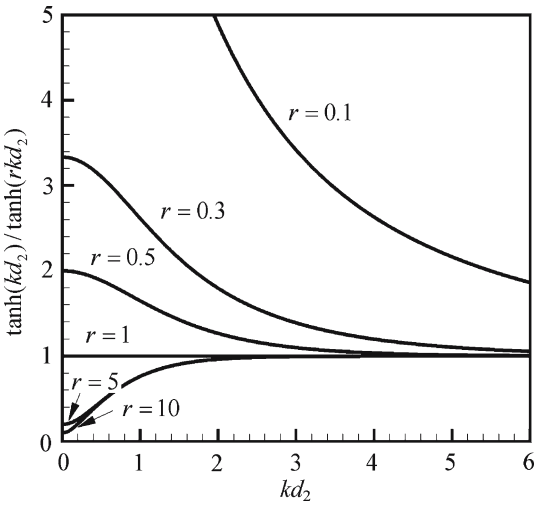

Fig. 4 Curves for $f(kd_2) = \tanh(kd_2)/\tanh(rkd_2)$ versus kd_2

the higher order waves. From Fig. 4, one can see that when $r < 1.0$, $f(kd) > 1.0$ and decreases monotonously with kd_2, while for $r > 1.0$, $0 < f(kd) < 1.0$. As for $r = 1.0$, the reduced density happens to be the Boussinesq parameter appearing in many articles [23,24].

3.4 Validity ranges of periodic wave theories

Now we are able to determine the validity ranges for various two-layer interfacial waves by using the above three criteria. The dispersion relation of the linear theory and the second order steady waves turns out,

$$\omega^2 = \frac{gk\sigma \cdot \tanh(kd_2)\tanh(kd_1)}{\tanh(kd_1) + (1-\sigma)\tanh(kd_2)} = gk \cdot F(kd_1, kd_2, \sigma). \tag{28}$$

We can get two co-correlative formulas as

$$\frac{H}{T^2} = \frac{g}{4\pi^2} \cdot kH \cdot F(kd_1, kd_2, \sigma), \tag{29}$$

$$\frac{d_2}{T^2} = \frac{g}{4\pi^2} \cdot kd_2 \cdot F(kd_1, kd_2, \sigma). \tag{30}$$

One important result of the second order theory is that the linear dispersion relation continues to hold. This considerably simplifies the application of the theory since the wave celerity and wavelength remain independent of the wave height. For the third order Stokes waves, the dispersion relation is

$$\frac{1}{T^2} = \frac{g}{4\pi^2} \cdot k \cdot (c_0 + \varepsilon c_1 + \varepsilon^2 c_2)^2, \tag{31}$$

where c_0 is expressed as Eq. (16) and $c_1 = 0$, c_2 is a function of ρ_1, ρ_2, d_1, d_2, k, etc. For the fourth order wave, Eq. (31) also keeps valid, so does the dispersion relation Eq. (13) for the fifth order. Now, the values of d_2/T^2 and H/T^2 corresponding to the given values of r and kd_2 may be determined by the direct computation. Just bearing in mind that the coefficient B_{22}, B_{33}, etc. are known functions of kd_2 and r, and then the solutions can be completed.

The current investigation comprises a systematic evaluation of the boundary condition fits for a number of wave theories over wave condition ranges of engineering significance. The parameters, H, T, d_2, and r uniquely define the characteristics of the period wave system propagating at the interface between two fluids of the given densities. The four parameters can be reduced into three independent dimensionless parameters, i.e., H/gT^2, d_2/gT^2 and r. It is more convenient and common to omit the gravitational term, resulting in the three parameters H/T^2, d_2/T^2 and r to define the characteristics of interfacial wave theories. The values of d_2/T^2 range from $5\times10^{-6}\,\mathrm{m/s^2}$ to $4\times10^{-3}\,\mathrm{m/s^2}$, which covers the most of engineering conditions of interest.

4 Validity ranges of cnoidal and solitary waves

4.1 Validity ranges of cnoidal waves

The function $f(x) = A\cos x + B\cos 2x$ with $|B/A|$ being 0.25 has a zero curvature point right at the wave trough or peak. For example, in the surface wave model, the wave profile formula of the second order Stokes waves can be written as

$$\eta = \frac{H}{2}\cos\theta + \frac{H}{8}\left(\frac{\pi H}{L}\right)\frac{\cosh(kd)}{\sinh^3(kd)}[2+\cosh(2kd)]\cos\theta. \tag{32}$$

According to the previous argument, zero curvature may occur at the wave trough when the magnitude ratio of the second term to the first one equals to 0.25 [25]. That is

$$\frac{H}{L} = \frac{1}{\pi}\frac{\tanh^3(kd)}{3-\tanh^2(kd)}. \tag{33}$$

If it is in shallow water, $3\tanh^2(kd)$ and $\tanh^3(kd)$ will tends to 3.0 and $(kd)^3$, respectively, therefore,

$$Ur = \frac{8}{3}\pi^2 \approx 26, \tag{34}$$

where Ur is defined as HL^2/d^3. For the two-layer internal waves, the wave profile formula of the second order is

$$k\eta(x) = \varepsilon\cos(kx) + \varepsilon^2 B_{22}\cos(2kx) + 0(\varepsilon^3). \tag{35}$$

The zero curvature point also exists if the absolute value of the amplitude ratio of the second term to the first one is 0.25, namely, $\varepsilon B_{22} = 1/4$. We have

$$kH = \frac{1}{2|B_{22}|}, \tag{36}$$

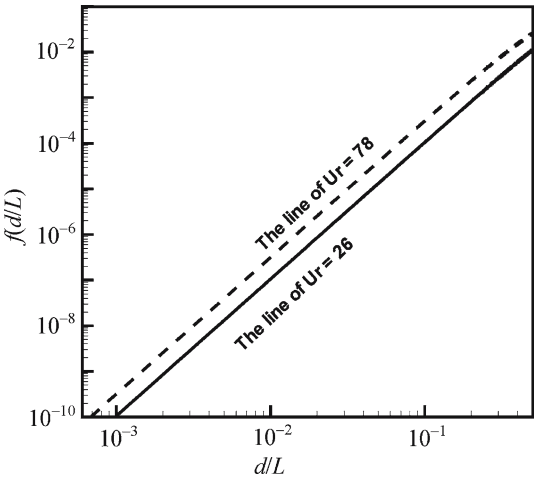

Fig. 5 Two lines of $Ur = 26$ and $Ur = 78$ which correspond to the surface waves and interfacial waves ($r = 1.0$), respectively. The figure indicates that the two lines are nearly parallel in the range of $d/L < 0.5$

which can be shown by the dashed line parallel to $Ur = 26$ in Fig. 5. If we move the former by multiplying d/L, then both of them may overlap. By try and error, we finally find that 1.44 is the right number we are looking for. Therefore, we have

$$\frac{H}{L} = \frac{1}{\pi}\frac{\tanh^3(1.44 \cdot kd_2)}{3 - \tanh^2(1.44 \cdot kd_2)}. \tag{37}$$

In this way, we get

$$Ur = \frac{1.44^3 HL^2}{(d_2)^3} \approx 78. \tag{38}$$

Consequently, the borderline of the cnoidal waves and the steady Stokes waves is $Ur = 78$ for $r = 1.0$ and 250 for $r = 10.0$. In the logarithm coordinate system of $d_2/T^2 - H/T^2$, the three curves of $Ur = 78, 250$ and $Ur = 26$ are very close to each other (see Fig. 6a) and so the validity range of various wave theories can be approximately regarded identical to some degree. Therefore, the curve of $Ur = 78$ can approximately serve as the borderline separating the two ranges of the internal Stokes and the cnoidal wave theories for $r > 1.0$.

4.2 Validity ranges of solitary wave theories

In determining the borderlines between the solitary waves and the cnoidal waves, the stream function theory can be used to separate the periodic waves and the non-periodic waves [21]. It is found that when the amplitude exceeds a certain limit, the periodic waves are no longer possible to depict the properties of the wave with huge wavelength and large period. Here we employ the same method in the study of the two-layer interfacial waves based on the solution obtained in Sect. 2, we get Ursell numbers of 0.006, 0.2, 1.0, 80, 200 and 500 for $r = 0.01, 0.05, 0.1, 0.5, 1.0, 10.0$, respectively, see Fig. 6b.

According to the assumption of no wave breaking, Holyer [17] and Saffman and Yue [26] performed extensive computation of the limiting configuration of the interfacial waves, demonstrating that when the interface profile is vertical at some point, the horizontal velocity at this point is equal to the phase speed. Tsugi and Nagta [27] assumed that before the limiting fluid velocity (which is larger than the phase speed) is reached, shear instability rather than convective instability for large amplitude internal waves might occur. This phenomenon was proved by Grue and Jensen [14] in experiments.

The horizontal component of fluid velocity for two-layer internal waves can be expressed as [10]

$$u_1 = c_0\eta_0/d_1, \tag{39}$$

$$u_2 = -c_0\eta_0/d_2, \tag{40}$$

the phase speed of the interfacial solitary wave is

$$c = c_0 + \alpha\eta_0/3, \tag{41}$$

and

$$\alpha = \frac{3c_0}{2d_1d_2}\left(\frac{d_1^2 - (1-\sigma)d_2^2}{d_1 + (1-\sigma)d_2}\right),$$

$$c_0 = \left[\frac{g\sigma d_1 d_2}{d_1 + (1-\sigma)d_2}\right]^{1/2},$$

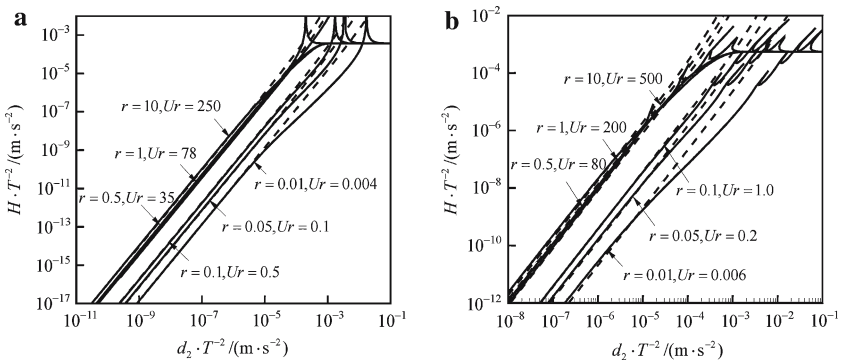

Fig. 6 The Ursell numbers used as the borderlines for various wave theories. **a** Borderlines between periodic wave theory and cnoidal theory. **b** Borderlines between solitary wave theory and cnoidal theory

if let $u_1 = c$ and $\eta_0 = H$ (suppose downward to be positive) when $r < 1.0$,

$$\left[\frac{1}{2d_2}\left(\frac{d_1^2-(1-\sigma)d_2^2}{d_1+(1-\sigma)d_2}\right)\right]\cdot\left(\frac{H}{d_1}\right)^2-\frac{H}{d_1}+1=0. \quad (42)$$

From Eq. (42) for $1.0 > r \geq 0.01$, the maximal value of H/d_1 we get is $0.67 < (H/d_1)_{\max} < 0.95$, it only has a little relation with the water depth ratio r.

If let $u_2 = c$ and $\eta_0 = -H$ when $r > 1.0$, we get

$$\left[\frac{1}{2d_1}\left(\frac{d_1^2-(1-\sigma)d_2^2}{d_1+(1-\sigma)d_2}\right)\right]\cdot\left(\frac{H}{d_2}\right)+\frac{H}{d_2}-1=0. \quad (43)$$

The maximal value of H/d_2 we get from the equation for all $100.0 > r > 1.0$ is $0.67 < (H/d_2)_{\max} < 0.99$.

For exploring the limiting steady waves, Grue and Jensen [14] studied the internal solitary waves propagating horizontally in a stratified two-layer fluid system. The fluid has a shallow layer with linear stratification while the densities of the upper and lower layers are kept constant. Their depths are defined as d_1 and d_2, and d_{thin} represents the thinner one of them. Grue and Jensen carried out both experiments and numerical simulation. It is found that when $a/d_{\text{thin}} = 0.855$, the fluid velocity at the interface is equal to the wave speed, and also the maximal horizontal fluid velocity is independent of r in the range of $d_1/d_2 = 0.5$–4.13. Grue's result is rather close to our computation $0.67 < (H/d_{\text{thin}})_{\max} < 0.99$, and is also similar to the conclusion by Long [28]. Considering Grue's result is based on the experiments, the steady maximal amplitude of two-layer internal solitary waves is 0.855. It is very close to the result of surface waves when the upper-layer is infinite deep.

The $K\mathrm{d}V$ equation we use arises from an assumption that weak nonlinearity, scaled by $(H'/l)^2 = O(a/H') \ll 1$. Here a is a measure of the wave amplitude, H' is an intrinsic vertical scale, and l is a measure of wavelength. For the observed highly nonlinear waves [29], using the $K\mathrm{d}V$ theory may induce that fluid velocity u_{max} exceeds the phase speed c. Their validity is determined by the criterion $\eta_{\max} = (d_1 - d_2)/2$. This criterion is pertaining to the MCC theory and the fully nonlinear theory.

5 Other borderlines

5.1 The curves of $Ur = \text{const}$

The curves of $Ur = \text{const}$ as an indication of the balance between the nonlinearity and the dispersion separate the ranges of all kinds of waves into sub-regions. Obviously, Ur is always less than 78 ($r = 1.0$) for the Stokes waves and larger than 500 ($r = 1.0$) for the solitary waves. According to the definition of Ursell number, we have

$$\lg(H/T^2) - \lg(d_2/T^2) = \lg Ur + 2\lg(kd_2/2\pi). \quad (44)$$

And from the Eq. (30), we can get the value of d_2/T^2. In this way, the curves for $Ur = \text{const}$ can be drawn in the $d_2/T^2 - H/T^2$ coordinates system. They turn out approximate straight lines.

5.2 The curves of $d_2/L = \text{const}$

According to the expression of the interfacial wave dispersion relation, we may find that the values of d_2/T^2 and d_2/L are corresponding to each other one by one. Therefore, the curves $d_2/L = \text{const}$ are all straight lines parallel to H/T^2 axis.

5.3 The curves of $H/d_2 = \text{const}$

$H/d_2 = \text{const}$, can be put in the form:

$$\frac{H/T^2}{d_2/T^2} = \text{const}. \quad (45)$$

Therefore, we have

$$\lg\left(\frac{H}{T^2}\right) = \lg\left(\frac{d_2}{T^2}\right) + \lg(\text{const}), \quad (46)$$

which shows that these curves are straight lines with slope being 1.0 in the logarithm coordinate system.

6 Discussion and conclusions

We have worked out a series of diagrams in Fig. 7, showing the validity ranges of various interfacial wave theories according to the wave parameters such as wave amplitude H, wavelength L, water depths d_1 and d_2 rather than a unique depth in the surface wave theory. Instead of appearing individually, all these wave parameters are combined together in the form of H/T^2 and d_2/T^2 (equivalently relative depth d_2/L). A particular wave steepness H/d_2 and $Ur = \text{const}$ are also used to play supplementary roles. As $r > 1.0$ in the domain of $d_2/L \geq 0.5$, it belongs to the deep-water range. The periodic wave theories are more appropriate in this circumstance, namely, the linear wave, the second to the fifth order wave theories can be correctly selected depending on a given wave steepness. The maximal values of H/T^2 for the five theories are 1.5×10^{-5}, 1.5×10^{-4}, 2.5×10^{-4}, 3.7×10^{-4} and 5.5×10^{-4}, respectively. However, the linear theory is bonded by $Ur = 20$ and $H/d_2 = 0.02$; the second order finite amplitude theory is limited by $Ur = 78$ and $H/d_2 = 0.2$; the third order wave between the lines of $Ur = 78$, $H/d_2 = 0.2$ and $H/d_2 = 0.4$; the fourth is between $H/d_2 = 0.4$ and $H/d_2 = 0.6$; the rest of the range is valid for the fifth or higher order waves ($r = 1.0$) in the

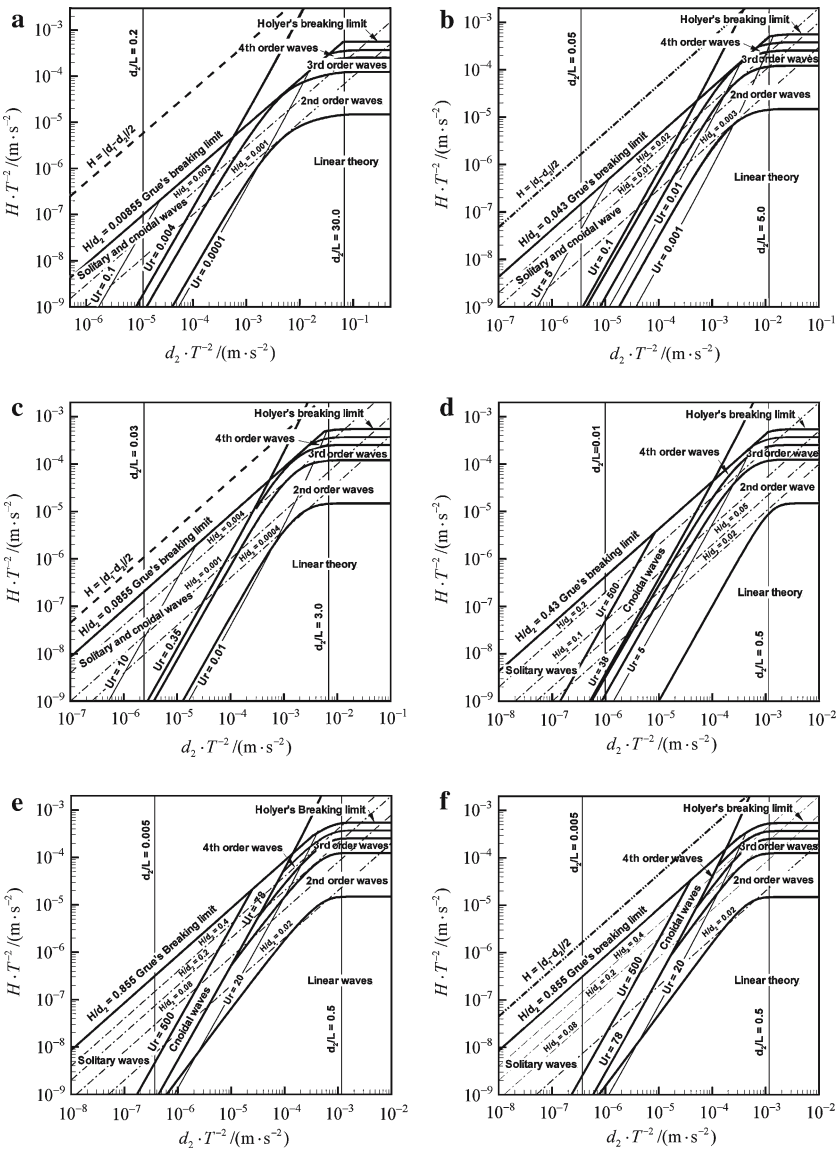

Fig. 7 The range of validity for various interfacial wave theories of two-layer fluid. From **(a)** to **(f)**, the water depth ratio r is equal to 0.01, 0.05, 0.1, 0.5, 1.0, and 10.0, respectively

intermediate water depth cases. We find that the higher order wave theory, the narrower the validity range. When the value of d_2/L becomes smaller, it corresponds to shallow water range. Then the finite amplitude long waves of permanent form are better described by the interfacial cnoidal and solitary wave theories. In Fig. 7 for $r = 1.0$, the validity ranges are bonded by $Ur = 78$ and $Ur = 500$. The two limiting cases are the solitary waves on one end of steep waves and the second order finite amplitude wave on the other end. As the wavelength becomes infinite, the solitary waves are approached, whereas the short wavelength yields the periodic wave theories in the limit.

Since wave breaking is usually not permitted for us, all the validity ranges should also be bounded by wave steepness lines. For example, $K\,\mathrm{d}V$ theory is bonded by Grue's breaking limit $H/d_{\mathrm{thin}} = 0.855$, which means that the maximal fluid velocity $u_{\max}$ is equal to the wave phase speed c. When the wave amplitude approximately exceeds the limit, Grue [14] has observed in experiments that wave breaking may take place with the wave speed $u_{\max}$ exceeding the phase speed c. As for the Stokes wave of various orders, the wave-breaking limit is that the steepness of the wave should be bounded by Hoyer's limit.

Let's examine the influences of the depth ratio r on the validity ranges. With the fixed wave amplitude and lower layer depth, the depth ratio indirectly affects the validity range by changing period. According to Eqs. (27) and (28), we find that for deep water, $f(kd)$ approaches to 1 and the effects of depth ratio r can be neglected. The results from all our computation are shown in Fig. 7, which shows that the curves in each of the charts are almost consistent to each other ($r \geq 1.0$). The figures exhibit a quite marked trend, and

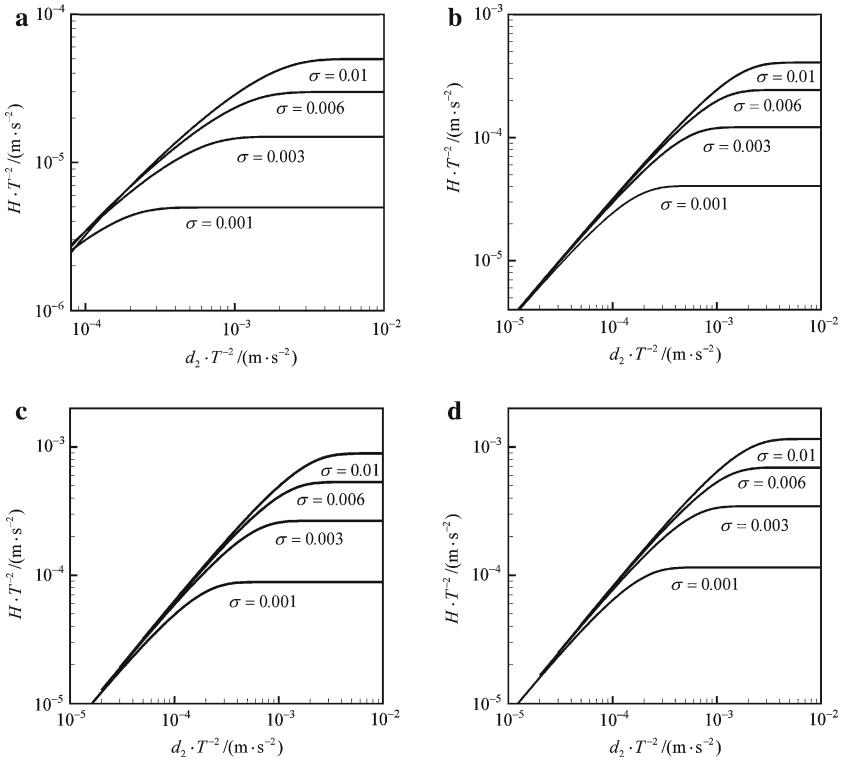

Fig. 8 The maximum amplitude of several internal steady waves at different σ. **a–d** Correspond to linear wave theory, the second to fourth order wave theories and σ are 0.001, 0.003, 0.006 and 0.01, respectively

the rough agreement between the ranges we get for different water depth ratios $r \geq 1.0$. However, we should consider the effect of depth ratio when the lower layer is not deep enough and $f(kd)$ deviates from 1.0.

Let's go on considering the fluid density effects on the validity ranges now. Just take the diagram for $r = 1.0$ as an example. As a matter of fact, different density ratios lead to different buoyancies, and then different gravity effects. As a result, the change in the relation between d_2/L and d_2/T^2 may change the whole validity range. Consequently, the water density ratio of the two layer fluids exerts non-negligible effect on the ranges of validity even when the density difference ratio alters just from 0.003 to 0.006 (see Fig. 8). With the increase of σ, the density changes may result in the decreasing of wave periods and wavelength. So the changes of H/T^2 and d_2/T^2 are large in the right horizontal coordinate comparable with the previous results. We may conclude that when $\sigma \to 1.0$, these lines of the interfacial waves will be consistent with the free surface limits. Accordingly, the values of Ursell numbers and H/d_2 will change with the increase of the density difference. The validity of the surface wave theories are obtained when $\sigma \to 1.0$ and $r \to \infty$, as shown in Fig. 9 (only the first four orders).

Since usual water surface wave can also be regarded as a two-layer system with upper atmosphere over lower water. Under this circumstance, the depth and the density ratio turn out infinity and 1.0, respectively. Therefore, the present theory is proposed in the current paper with foregoing parameters, we should resume the results for the water surface wave. That is, the diagram will be identical to the Le Méhauté's. On the other hand, the Le Méhauté's diagram can be used for the interfacial wave theories if the reduced gravity replaces the conventional gravity ($r \geq 1.0$).

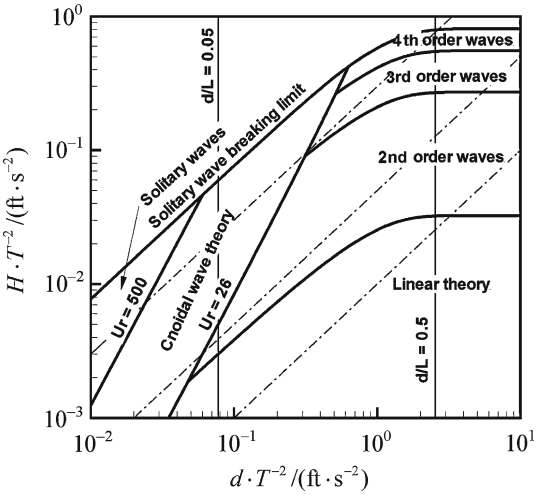

Fig. 9 The validity ranges of surface wave theories when $\sigma \to 1.0$ and $r \to \infty$, and using the English unit to compare with Le Méhauté's results

We have provided a diagram of the validity range for the interfacial wave theories, which may facilitate engineers and scientists to select an appropriate wave theory for the flow

field and the wave loading calculation. In addition, if r is small enough, the free surface effect can never be neglected, which should be paid attention to the future research.

References

1. Cai, S.Q., Long, X.M., Gan, Z.J.: A numerical study of the generation and propagation of internal solitary waves in the Luzon Strait. Oceanol. Acta **25**, 51–60 (2002)
2. Ablowitz, M.J., Clarkson, P.A.: Solitons, Nonlinear Evolution Equations and Inverse Scattering. Cambridge University Press, Cambridge (1991)
3. Osbourne, A.R., Burch, T.I.: Internal solitons in the Andaman Sea. Science **208**(4443), 451–460 (1980)
4. Ebbesmeyer, C.C., Coomes, C.A., Hamilton, R.C. et al.: New observation on internal wave in the South China Sea using an acoustic Doppler current profiler. In: New Orleans: Marine Technology Society 91 Proceedings, pp. 165–175 (1991)
5. Le Méhauté, B.: An Introduction to Hydrodynamics and Water Waves, pp. 204–205. Springer, New York (1976)
6. Yuen, H.C., Lake, B.M.: Nonlinear Deep Water Waves: a Physical Testing Ground for Solitons and Recurrence, Significance of Nonlinearity in Natural Science, pp. 67–96. Plenum Press, New York (1977)
7. Chakrabarti, S.K.: Laboratory generated waves and wave theories. J. Waterway Port Coastal Ocean Division **106**(3), 349–368 (1980)
8. Iwagaki, Y.: New coastal engineering, pp. 54–55. Morikita–Shuppan (1987)
9. Cheng, Y.L., Li, J.C.: An LS. Stokes 5th order internal wave and its action on cylindrical piles. In: Proceeding of 16th ISPE, pp. 459–466. Los Angles, CA (2006)
10. Lamb, K.G., Wan, B.: Conjugate flows and flat solitary waves for a continuously stratified fluid. Phys. Fluid **10**, 2061–2079 (1998)
11. Helfrich, K.R., Melville, W.K.: Long nonlinear internal waves. Annu. Rev. Fluid Mech. **38**, 395–425 (2006)
12. Miyata, M.: Long internal waves of large amplitude. In: Horikawa, H., Maruo, H. (eds.) Proceedings of the IUTAM Symposium on Nonlinear Water Waves, pp. 399–400. Tokyo, Japan (1988)
13. Choi, W., Camassa, R.: Fully nonlinear internal waves in a two–fluid system. J. Fluid Mech. **396**, 1–36 (1999)
14. Michallet, H., Barthelemy, E.: Experimental study of interfacial solitary waves. J. Fluid Mech. **366**, 159–177 (1998)
15. Grue, J., Jensen, A., Rusaas, P.O., Sveen, J.K.: Breaking and broadening of internal solitary waves. J. Fluid Mech. **413**, 181–217 (2000)
16. Fringer, O.B., Street, R.L.: The dynamics of breaking progressive interfacial waves. J. Fluid Mech. **494**, 319–353 (2003)
17. Holyer, J.Y.: Large amplitude progressive interfacial waves. J. Fluid Mech. **93**, 433–434 (1979)
18. Kao, T.W., et al.: Internal solitons on the pycnocline: generation, propagation, and shoaling on breaking over a slope. J. Fluid Mech. **159**, 19–53 (1985)
19. Benney, D.J.: Long non-linear waves in fluid flows. J. Math. Phys. **45**, 52–63 (1966)
20. Pelinovskiy, E.N., Talipova, T.G.: Scaling effects in the modeling of internal waves in basin covered by surfactant films. Atmos. Oceanic Phys. **31**(5), 672–675 (English Translation) (1996)
21. Sarpkaya T. (1981) Mechanics of Wave Forces on Offshore Structures, pp. 215–218. van Nostrand Reinhold Co., New York
22. Magdi, H.R., Denny, R.S.K.: Interaction between small-scale surface waves and large scale internal waves. Phys. Fluid **21**(11), 1900–1907 (1978)
23. Gear, J.A, Grimshaw, R.H.: A second-order theory for solitary waves in shallow fluids. Phys. Fluid **26**(1), 14–26 (1983)
24. Lighthill J. (1978) Waves in Fluids, pp. 284–432. Cambridge University Press, Cambridge
25. Clauss, G., Lehmann, E., Ostergaard, C.: Offshore Structures, vol. 1, pp. 164–165, pp. 189–190, Springer, New York (1992)
26. Saffman, P.G., Yuen, H.C.: Finite-amplitude interfacial waves in the presence of a current. J. Fluid Mech. **123**, 459–476 (1982)
27. Tsugi, Y., Nagata, Y.: Stokes' expansion of internal deep-water waves to the fifth order. J. Oceanogr. Soc. Japan **29**, 61–69 (1973)
28. Long, R.R.: Solitary waves in one and two-fluid systems. Tellus **8**, 460–471 (1956)
29. Duda, T.F., Lynch, J.F., Irish, J.D., et al.: Internal tide and nonlinear wave behavior in the continental slope in the northern South China Sea. IEEE J. Ocean Eng. **29**, 1105–1131 (2004)